



Published in final edited form as:

*J Med Chem.* 2012 June 28; 55(12): 5749–5759. doi:10.1021/jm300338m.

## Life Beyond Kinases: Structure-based Discovery of Sorafenib as Nanomolar Antagonist of 5-HT Receptors

Xingyu Lin<sup>1,2</sup>, Xi-Ping Huang<sup>3</sup>, Gang Chen<sup>4</sup>, Ryan Whaley<sup>3</sup>, Shiming Peng<sup>1</sup>, Yanli Wang<sup>1</sup>, Guoliang Zhang<sup>4</sup>, Simon X. Wang<sup>5</sup>, Shaohui Wang<sup>4</sup>, Bryan L. Roth<sup>3</sup>, and Niu Huang<sup>1,\*</sup>

<sup>1</sup>National Institute of Biological Sciences, Beijing, No. 7 Science Park Road, Zhongguancun Life Science Park, Beijing 102206, China

<sup>2</sup>College of Life Sciences, Beijing Normal University, No. 19 Xijiekouwai St, Beijing 100875, China

<sup>3</sup>Department of Pharmacology and Division of Medicinal Chemistry and Natural Products, The University of North Carolina, Chapel Hill, North Carolina 27759, USA

<sup>4</sup>BeiGene (Beijing) Co., Ltd., No. 30 Science Park Road, Zhongguancun Life Science Park, Beijing 102206, China

<sup>5</sup>Department of Pharmaceutical Sciences, Howard University, Washington DC, 20059, USA

### Abstract

Of great interest in recent years has been computationally predicting the novel polypharmacology of drug molecules. Here, we applied an “induced-fit” protocol to improve the homology models of 5-HT<sub>2A</sub> receptor, and we assessed the quality of these models in retrospective virtual screening. Subsequently, we computationally screened the FDA approved drug molecules against the best induced-fit 5-HT<sub>2A</sub> models, and chose six top scoring hits for experimental assays. Surprisingly, one well-known kinase inhibitor, sorafenib has shown unexpected promiscuous 5-HTRs binding affinities,  $K_i = 1959, 56$  and  $417$  nM against 5-HT<sub>2A</sub>, 5-HT<sub>2B</sub> and 5-HT<sub>2C</sub>, respectively. Our preliminary SAR exploration supports the predicted binding mode, and further suggests sorafenib to be a novel lead compound for 5HTR ligand discovery. Although it has been well known that sorafenib produces anticancer effects through targeting multiple kinases, carefully designed experimental studies are desirable to fully understand whether its “off-target” 5-HTR binding activities contribute to its therapeutic efficacy or otherwise undesirable side effects.

### Keywords

GPCR; 5-HTR; induced-fit; molecular docking; molecular dynamics; sorafenib

## 1. INTRODUCTION

Currently, target-based drug discovery is typically defined as “one compound - one target - one disease” with the idea that deliberately designed single-target drugs may hold the

\*Corresponding Author: N. H. Phone: 86-10-80720645. Fax : 86-10-80720813. huangniu@nibs.ac.cn.

Supporting Information Available: The Sequence alignment between 5-HT<sub>2A</sub> and its template  $\beta$ -2 adrenoceptor, the structural descriptors used to evaluate the ketanserin complex system, the chemical structure and docking pose prediction assessment of ketanserin-like and cyproheptadine-like ligands, the ranks and annotated activities of top scored docking hits, the structures and experimental binding data of six FDA approved drugs, the detailed experimental assay protocols, and the chemical synthesis route for sorafenib analogues and their corresponding analysis data. This information is available free of charge via the Internet at <http://pubs.acs.org>.

promise to specifically bind their target with reduced side effects due to off-target actions. However, single-target drugs often turn out to be less effective in treating complicated diseases such as cancers, metabolic disorders and central nervous system (CNS) diseases.<sup>1, 2</sup> Furthermore, many compounds designated as target-specific drugs are in fact not that selective, and subsequently have been discovered to bind to other targets with similar binding affinities.<sup>3-5</sup> To better and more efficiently identify effective compounds that work through either known or undiscovered mechanisms, of great interest in recent years has been the development of computational methods to predict the promiscuous binding propensities of drug molecules.<sup>6-9</sup>

G protein-coupled receptors (GPCRs) and kinases are two of the most important drug target families. Many of their ligands are well known to have promiscuous binding propensities within their own protein families. For example, as one of the most efficacious atypical antipsychotic drugs discovered half a century ago, clozapine binds to dozens of GPCRs with nM affinity<sup>10</sup> and its clinical efficacy is certainly associated with its broad target binding profile.<sup>1, 10</sup> Similarly, the first “magic bullet” approved by the FDA for the treatment of chronic myeloid leukemia, gleevec, was initially developed to specifically inhibit the abnormal tyrosine kinase BCR-ABL. However, it was shown subsequently to target several other kinases simultaneously, including c-KIT and PDGFR.<sup>4, 5</sup> Historically, GPCR ligands and kinase inhibitors have been developed in quite distinct chemical spaces,<sup>11</sup> and the selectivity panel screening campaign has generally been limited to within the same protein family members. Thus, as far as we are aware, the ligand cross-reactivity between GPCR orthosteric ligands and kinase inhibitors has not been previously reported.

The 5-hydroxytryptamine receptors (5-HTRs) are comprised of 14 GPCRs in 5 families (5-HT<sub>1</sub>, 2, 4, 5, 6 and 7) and one ligand-gated ion channel (5-HT<sub>3</sub>). Among 5-HTRs, the 5-HT<sub>2A</sub> receptor is one of the most studied serotonergic receptors, and its inhibition is generally associated with antipsychotic and antidepressive effects.<sup>12</sup> In addition, the 5-HT<sub>2A</sub> receptor also plays a role in thermoregulation, sleep, cardiovascular function and muscle contraction.<sup>13-17</sup> A typical 5-HT<sub>2A</sub> antagonist consists of two aryl rings and a positively charged nitrogen atom (Figure 1), and generally can be divided into class I antagonists characterized by a basic nitrogen atom in the center of the molecule and in linear disposition with the aryl rings (e.g. ketanserin), or class II antagonists with a triangular arrangement of aryl rings and a basic nitrogen (e.g. cyproheptadine).<sup>18</sup> Currently, very few 5-HTR ligands are subtype-selective, and the development of novel 5-HT antagonists with better specificity is highly desirable. However, this has been compromised by the lack of experimental structures of 5-HTRs.

High resolution crystal structures of GPCRs have been published in recent years,<sup>19</sup> in addition to the pioneering structures of rhodopsin,<sup>20</sup> which greatly facilitates the GPCR structure-function study and drug discovery.<sup>19, 21</sup> Much research is now engaged in using the available structural information for homology modeling the 3D structures of GPCRs, and subsequently for docking screening and lead compound optimization purposes.<sup>22-27, 28, 29</sup>

Here we combine homology modeling, molecular docking and molecular dynamics simulation methods to predict the potential 5-HT<sub>2A</sub> off-target activity of FDA approved drugs, which has not been investigated previously. We employed an “induced-fit” protocol to simulate the receptor conformational changes upon binding with two representative 5-HT<sub>2A</sub> antagonists. We asked whether such induced-fit models can be used to enrich known ligands from decoy molecules in retrospective virtual screening. We then asked whether we could discover potential novel polypharmacology in a prospective docking screening of FDA drug molecules.

## 2. METHODS

### 5-HT<sub>2A</sub> Comparative Modeling

The crystal structure (PDB code: 3D4S)<sup>30</sup> of the inverse agonist bound  $\beta$ 2-adrenoceptor ( $\beta$ 2-AR) was chosen as template to model the inactive 5-HT<sub>2A</sub> structure using the comparative modeling program MODELLER (version 9v7).<sup>31</sup> The  $\beta$ 2 receptor has higher homology with the 5-HT<sub>2A</sub> receptor than with rhodopsin and has been suggested as a better template for homology modeling.<sup>25</sup> The sequence alignment was retrieved from GPCRDB<sup>32</sup> and CDD database<sup>33</sup> with the extracellular loop 2 (ECL2) included and the conserved disulfide bond patched, while four residues at the N terminal and five residues at the C terminal of the third intracellular loop were treated as gaps in sequence alignment to avoid the generation of linkage between transmembrane helix (TM) 5 and TM6 during structure prediction (Figure S1 in Supplementary Material). The best quality model was identified with most residues located in the favored regions assessed by Ramachandran plot using Maestro (*Schrödinger* LLC, New York NY). The ECL2 loop and the third intracellular loop were deleted after the generation of the homology model to avoid interference from the less accurately modeled loops to the subsequent molecular docking and MD simulation. The same strategy has been applied in other GPCR modeling projects.<sup>34, 35</sup>

### Binding-site Refinement

Instead of docking to the comparative model directly, we deliberately modified the receptor structure to incorporate knowledge of “induced-fit” effects associated with varying 5-HT<sub>2A</sub> antagonists’ scaffolds.<sup>36, 37</sup> Although 5-HT<sub>2A</sub> ligands are structurally quite diverse, the majority of 5-HT<sub>2A</sub> antagonists belong to class I and class II antagonists. Specifically, we chose ketanserin as the representative ligand of class I antagonist and cyproheptadine as class II antagonist, and we applied an induced-fit protocol (Figure 2) to sample the receptor conformational changes upon binding ketanserin and cyproheptadine, respectively.

The ligand was docked into the modeled 5-HT<sub>2A</sub> binding-site using the DOCK 3.5.54 program, a flexible-ligand method that uses a force-field-based scoring function.<sup>38, 39</sup> The ligand binding-site residues were defined as in a consensus aminergic binding-site residue set, which includes 12 residues on TM3 (3.32, 3.33, 3.37 and 3.40), TM5 (5.42, 5.43, 5.46 and 5.47), TM6 (6.51 and 6.52), and TM7 (7.42 and 7.43).<sup>40</sup> We adopted the default parameter settings from an automated docking platform as described previously<sup>41–43</sup>, in which all tasks including sphere generation, scoring grid and docking calculations are driven automatically, and the same docking protocol was used in the subsequent docking screenings. At this step, we saved all the docking poses for further structural analysis.

Docking poses of ketanserin and cyproheptadine were filtered by the 5 Å distance criteria between the positively charged nitrogen atom of the ligand and negatively charged carboxylate oxygen atom of D<sub>3.32</sub>. The resulting poses were clustered into dissimilar structural groups using the DBSCAN algorithm<sup>44</sup> where the minimum spanning number was set to 5 or 10 points and a RMSD cutoff value of 1.5 or 2 Å for cyproheptadine and ketanserin, was applied individually. One single representative docking pose was identified from each structural cluster by choosing the most highly ranked pose that exhibits a reasonable binding mode in the binding-site. Finally, twelve diverse docking poses were selected for ketanserin, and four for cyproheptadine.

We submitted the selected dissimilar docking poses to a MM-GB/SA refinement and rescoring procedure<sup>45–50</sup>, where the side chain of binding-site residues were sampled along with the docked ligand using Protein Local Optimization Program (PLOP).<sup>51–53</sup> Note that in our previously published works, the protein was kept rigid during minimization of the ligand-protein complex; here, we attempted to sample the side chain conformational changes

with the presence of the docked ligand.<sup>28, 36, 50</sup> The docked complex structure was minimized first, followed by the side chain prediction of the binding-site residues within 5 Å of the ligand, and then the ligand was minimized with the fixed protein structure. The binding-site “induced-fit” complex structure was utilized as the starting point for further global structure refinement via molecular dynamics (MD) simulation including explicit lipid membrane and water environment.

### Global “Induced-fit” via MD Simulation

All molecular dynamic simulations were performed using the Desmond software package<sup>54</sup> and the OPLS-AA 2005 force field.<sup>55</sup> Using the default Schrödinger protein membrane building protocol, a 10 Å buffered orthorhombic boundary system was built with a POPC lipid membrane and SPC water and then neutralized by ions. The default Schrödinger protein membrane equilibration protocol was applied before production run. Briefly, each system was minimized using 2000 steps of steepest descent algorithm, followed by L-BGFS algorithm. Temperature was gradually increased from 0 K to 300 K, while 50 kcal·mol<sup>-1</sup>·Å<sup>-2</sup> harmonic position restraints were applied to all heavy atoms of the protein and ligand during system equilibration. The restraints were gradually removed and the production run was performed in MTK-NPT (1 bar, 300 K) ensemble for 20 ns. The M-SHAKE algorithm<sup>56</sup> was applied to constrain all bonds involving hydrogen atoms with a time step of 2 fs. The short-range electrostatic and Lennard-Jones interactions were cut off at 9 Å. Long-range electrostatic interactions were computed by the Particle Mesh Ewald (PME) method<sup>57</sup> using 64×64×64 grid with  $\sigma$  equal to 2.18 Å. Analysis of the MD simulations focused on structural and energetic properties averaged over the 10 ns production simulation. Structural analysis was performed using the UCSF Chimera<sup>58</sup> and VMD<sup>59</sup> programs, including standard root-mean-square differences (RMSDs), atom contacts and hydrogen bonding analysis.

### Model Assessment by Retrospective Docking Screening

We next investigated the ability of our induced-fit models to enrich known ligands of the 5-HT<sub>2A</sub> receptor. Forty-three structurally diverse 5-HT<sub>2A</sub> antagonists were collected from references, and molecules were prepared for docking using the latest version of the ZINC protocol.<sup>60</sup> Twenty decoy compounds were selected for each ligand from an in-house screening compound library (170,000 compounds) based on the DUD protocol,<sup>41</sup> leading to a total of 774 non-redundant decoys that were physically similar but topologically dissimilar to the 43 annotated ligands (both ligands and decoy molecules are available at <http://www.huanglab.org.cn/5-HT2A>). Our automatic docking screening protocol was applied in default setting for each modeled receptor structure. Enrichment performance represents the prioritization of ligands among the top ranks of a docking-ordered library. We assessed the quality of the twenty induced-fit models by the early enrichment of annotated ligands from a background of decoy molecules..

### Prospective Virtual Screening of FDA Drugs

We compiled a FDA drug library by merging the drug molecules from DrugBank (version 2.0)<sup>61</sup> and ZINC FDA drug subset (version 2005)<sup>60</sup> with excluding the molecules with molecular weight larger than 600 or smaller than 100 dalton. A total of 1430 unique molecules were screened against two receptor models by applying our automatic docking and MM-GB/SA rescoring protocol, individually.<sup>47-49</sup> Note that only a single docking pose with the best total docking energy score was rescored for each molecule entry to reduce the computation cost, ultimately, we will test the docking screening capacity to rescore multiple docking poses by including the receptor binding-site flexibility. We saved the top 200 hits from MM-GB/SA scoring method for further structural analysis and visual check.

To simulate the stringent scenario with which to discover potential novel polypharmacology, we excluded the top scoring molecules with any potential GPCR-related activities, such as ligands of mono-amine GPCRs, mono-amine transporters and opioid receptors. All the activity data was retrieved from publicly available resources, including ChEMBL database<sup>62</sup> and DrugBank.<sup>61</sup> In addition, we also submitted identified hits to the Similarity Ensemble Approach (SEA, <http://sea.bkslab.org/>) server to avoid the selection of structurally similar compounds of known GPCR ligands.<sup>7, 63</sup> SEA makes use of the chemical fingerprints of annotated ligands, calculates the similarity score between each set of ligands, and ranks the significance of the similarity scores using a rigorous statistical model.

### Experimental Assays

The detailed description of experimental assays is included in the Supplementary Materials. Briefly, the experimental binding assays were performed by the National Institute of Mental Health's Psychoactive Drug Screening Program (PDSP) following the standard protocol. The radio-labeled reference compounds (<sup>3</sup>H]8-OH-DPAT for 5-HT<sub>1A</sub>; [<sup>3</sup>H]GR127543 for 5-HT<sub>1B</sub> and 5-HT<sub>1D</sub>; [<sup>3</sup>H]5-HT for 5-HT<sub>1E</sub>; [<sup>3</sup>H]Ketanserin for 5-HT<sub>2A</sub>; [<sup>3</sup>H]LSD for 5-HT<sub>2B</sub> and 5-HT<sub>2C</sub>, 5-HT<sub>5a</sub>, 5-HT<sub>6</sub> and 5-HT<sub>7</sub>; [<sup>3</sup>H]LY278584 for 5-HT<sub>3</sub>) are used in Ki determination. The PDSP on-line data entry and analysis system calculates the variance of the quadruplicate determinations (for the total, non-specific, and test compound binding values) and variances greater than 20% are flagged for further inspection and assays are repeated if necessary.

## 3. RESULTS AND DISCUSSION

### 5-HT<sub>2A</sub> Induced-fit Models upon Binding with Ketanserin and Cyproheptadine

Previous computational studies have demonstrated that incorporating ligand information, binding-site residue mutation data and molecular dynamics simulations improves the quality of GPCR structure prediction and ligand docking.<sup>26</sup> It is likely that the receptor undergoes conformational changes to accommodate different ligands, and rigid docking against one particular receptor conformation may be of limited utility in identifying a diverse set of ligands. The majority of 5-HT<sub>2A</sub> antagonists belong to class I and class II antagonists, therefore, we choose ketanserin and cyproheptadine to represent the typical 5-HT<sub>2A</sub> antagonists. We systematically improved the homology model in the context of these two ligands, and we assessed the extent of such ligand-induced conformational differences and revealed further details of ligand binding. We expect that the binding modes of class I and class II antagonists are similar to ketanserin and cyproheptadine, respectively.

Although the position of the orthosteric ligand binding-site is conserved in the aminergic GPCRs, the detailed atomic interactions with binding-site residues vary quite considerably.<sup>40</sup> It has been suggested that 5-HT<sub>2A</sub> ligands may bind into two different sites.<sup>64, 65</sup> Site 1 is bordered by TM3, 4, 5 and 6, and site 2 is flanked by TM1, 2, 3 and 7. The shared region between site 1 and site 2 includes residues D<sub>3.32</sub> and S<sub>3.36</sub> on TM3, and W<sub>6.48</sub> and F<sub>6.51</sub> on TM6.<sup>65</sup> In aminergic GPCRs, the conserved D<sub>3.32</sub> forms a salt-bridge with the tertiary amine of the ligand, which is critical for ligand binding<sup>66</sup>. Therefore, we generated a wide range of docking poses at the initial docking stage, followed by eliminating the misdocked poses using the conserved salt-bridge interaction as a criterion. Further structural clustering significantly reduced the redundant docking poses, and eventually led to twelve dissimilar poses for ketanserin and four poses for cyproheptadine. Consistent with previous suggestions, our docking results indicate that ketanserin adopts extended conformations that allow binding in both sites, while cyproheptadine mainly binds in site 1 (Figure 3). The binding-site refinement procedure didn't introduce large structural perturbation; however, the sidechain prediction within the binding pocket along with the



docked ligand is an effective approach to maximize the interactions between binding-site residues and docked ligand, and thus provides a physically reasonable complex structure for subsequent molecular dynamics simulation.

Based on docking and refinement results alone, it is difficult to determine the correct binding orientation for ketanserin. The anchoring interaction is the salt bridge between the piperidine basic nitrogen of the ligand with carboxylate group of D<sub>3.32</sub>; however, it appears reasonable that either the p-fluorobenzoyl ring or quinazolinedione moiety binds in site 1 (Figure 3). Therefore, this limitation stimulated the development of the improved protein-ligand complex models in a more realistic treatment using the unbiased molecular dynamics simulation approach. We expect that multiple independent simulations can significantly increase the sampling of the complex structure, and the near-native system will be the stable system with favorable interactions between ligand and receptor, and satisfies the experimental evidences like site-directed mutagenesis data.

In addition to the critical residue D<sub>3.32</sub>, the binding-site residues important for ketanserin binding have been extensively studied by mutagenesis experiments. The F<sub>6.51</sub>L mutant decreases ketanserin binding by at least 800-fold and the W<sub>6.48</sub>A mutant decreases only 7-fold, while S<sub>3.36</sub>A/C and F<sub>6.52</sub>L mutations were found to have almost no effect on ketanserin binding affinity.<sup>67-70</sup> Structure-activity relationship (SAR) studies on ketanserin analogues have been shown that the hydrogen bonding capability of the quinazolinedione ring has only minor contributes to the binding affinity.<sup>71</sup> Furthermore, it is suggested that an ionic lock (R<sub>3.50</sub> And E<sub>6.30</sub>) forms in aminergic GPCRs to stabilize the receptor in an inactive conformation.<sup>20</sup> Also, conserved residue Y<sub>7.43</sub> forms a stable hydrogen bond with D<sub>3.32</sub> in all known GPCR crystal structures. Therefore, we defined six structural descriptors to assess the simulation quality of each ketanserin system during the last 10 ns simulation, including the formation of salt bridge interaction between ternary amine of ligand and conserved residue D<sub>3.32</sub>, the absence of hydrogen bond between ligand and hydroxyl of residue S<sub>3.36</sub>, larger ratio of vdw contacts between ligand and Phe<sub>6.51</sub> in comparison to Trp<sub>6.48</sub> and Phe<sub>6.52</sub>, the formation of conserved ionic lock between R<sub>3.50</sub> and E<sub>6.30</sub> residues and the presence of a stable hydrogen bond between Y<sub>7.43</sub> and D<sub>3.32</sub>. We also compared the average MM-GBSA binding energies of different systems. A single simulation system (designated as Ket-6) was eventually chosen on the basis of satisfying all these available experimental evidences and energetic calculation results while the rest of systems do not agree with at least one of the descriptors (Figure 4), the detailed analysis are also summarized in the Supplementary Materials (Table S1).

In the Ket-6 system (Figure 5A), the p-fluorobenzoyl moiety binds in site 1, forming favorable hydrophobic interaction with F<sub>6.51</sub>, but relatively fewer contacts with W<sub>6.48</sub> and F<sub>6.52</sub>. The quinazolinedione group binds in site 2, establishing aromatic stacking interaction with W<sub>3.28</sub> without forming any stable hydrogen bonds in the binding-site; the positively charged piperidine nitrogen forms strong salt bridge interaction with D<sub>3.32</sub> throughout the entire simulation, and S<sub>3.36</sub> only interacts transiently with the carbonyl group of the p-fluorobenzoyl ring. Nevertheless, the last 10 ns simulation trajectory in the Ket-6 simulation was clustered, a representative structure from each of the 10 largest conformational ensembles was selected, and resulted total of 10 representative model structures for docking evaluation.

Because of its relatively rigid structure, determination of the binding mode of cyproheptadine is less uncertain. We still assess the simulation quality using the conserved salt bridge interaction between the positively charged nitrogen of the ligand and D<sub>3.32</sub>, as well as the ionic lock between R<sub>3.50</sub> and E<sub>6.30</sub> and the hydrogen bond between D<sub>3.32</sub> and Y<sub>7.43</sub>. Only one simulation system (designated as Cyp-4) satisfies the structural

requirements (data not shown), and additionally exhibits more favorable hydrophobic interaction between the bound ligand and binding-site residues (Figure 5B). Cyproheptadine mainly binds in site 1 deeply; forming strong hydrophobic interaction with V<sub>3.33</sub>, F<sub>5.38</sub>, W<sub>6.48</sub>, F<sub>6.51</sub> and F<sub>6.52</sub>, while maintaining its critical ionic interaction with D<sub>3.32</sub>. Similarly, we clustered the last 10 ns simulation trajectory in the Cyp-4 simulation, and selected a representative structure from each of the 10 largest clusters for docking evaluation.

### Assessing Induced-fit Models by Retrospective Docking Screening

We next investigate the docking enrichment performance of a total of twenty 5-HT<sub>2A</sub> induced-fit models. The early enrichment results are presented using EF<sub>1</sub> (enrichment factor at 1% of the ranked database) and EF<sub>5</sub> (enrichment factor at 5% of the ranked database) (Table 1). The best early enrichment performances are achieved for the 7<sup>th</sup> representative structure from the Ket-6 simulation (designated as Ket-6-7) with EF<sub>1</sub> of 4.6 and EF<sub>5</sub> of 2.3, and for the 4<sup>th</sup> representative structure from the Cyp-4 simulation (designated as Cyp-4-4) with EF<sub>1</sub> of 4.6 and EF<sub>5</sub> of 3.3, respectively. During the docking screening, it was frequently observed that one class of ligand was favored over others, indicating that different receptor conformations may be required for extensive virtual screening studies, which is exactly the case in our study. Thus, we further extracted two subsets of antagonists as ketanserin-like set and cyproheptadine-like set on the basis of structural similarity (Table S2 in Supplementary Materials), and we expected that the ketanserin-like ligands should be better enriched by the corresponding ketanserin induced-fit models, and similarly in cyproheptadine cases. Indeed, the early enrichment was significantly improved for the same group of ligands against the corresponding induced-fit models (Figure 6). Thus, 16.7% and 25% of the ketanserin-like ligands can be found in the top 1% and 5% of the ranked database by docking against Ket-6-7 model, respectively, corresponding to enrichment factors of 16.7 and 5. A significantly better enrichment occurs when docking against Cyp-4-4 model, as 25% and 58.3% of the cyproheptadine-like ligands are found in the top 1% and 5% of the docking ranked database, corresponding to enrichment factors of 25 and 11.7.

We were also interested in comparing the docking enrichment performance of two induced-fit models to the initial comparative model and to a previously published 5-HT<sub>2A</sub> induced-fit model structure.<sup>28</sup> Clearly, enrichments are much better in docking screening against our induced-fit models than the original homology model and one published model using exactly the same group of ligands and decoy molecules (Figure 6). In addition, we visually checked the docking poses of these ligands based on the assumption that the binding modes of class I and class II antagonists shall be similar to ketanserin and cyproheptadine, respectively. Our results (Table S2) demonstrate that the ligand docked to its corresponding induced-fit model typically superimposes well with its reference molecule (91% success rate for cyproheptadine-like ligands and 73% for ketanserin-like ligands), while the binding orientation by docking to the initial homology model is frequently incorrect (only 45% and 36% of success rate, correspondingly). It was encouraging that our induced-fit models are reliable for typical 5-HT<sub>2A</sub> antagonist binding geometry prediction and enrichment studies, and we are confident that the same induced-fit protocol can be applied to model 5-HT<sub>2A</sub> atypical antagonist bound conformations. Nevertheless, the Ket-6-7 and Cyp-4-4 models, each corresponding to one class of 5-HT<sub>2A</sub> ligands, were chosen for subsequent docking screening of FDA drug molecules. The structural coordinates of both induced-fit models are freely available online (<http://www.huanglab.org.cn/5-HT2A>).

### Prospective Virtual Screening of FDA Drugs and Experimental Validation

We then docked FDA drug molecules against both modeled 5-HT<sub>2A</sub> structures and checked the top 200 compounds based on MM-GB/SA energy scores. For the present study, we mainly focused on analyzing and testing the docking results from Cyp-4-4 model due to its

better enrichment performance and pose fidelity prediction in our retrospective virtual screening. Firstly, we filtered out compounds without forming favorable hydrogen bonding interaction with residue Asp<sub>3.32</sub>, resulting in 99 remaining molecules. Unsurprisingly, 73 molecules among these 99 compounds belong to annotated ligands of monoaminergic GPCRs, opioid GPCRs or their corresponding membrane transporters (Table S3), such as phentolamine (ranking 10,  $\alpha$  adrenergic receptor blocker), mesoridazine (ranking 14, 5-HT<sub>2A</sub> and D2 receptor antagonist) and epinastine (ranking 27, histamine receptor antagonist). The aminergic GPCRs share the same or similar cognate ligands such as serotonin, dopamine and epinephrine, and drugs targeting these receptors display broad cross-reactivity. Therefore, we eliminated all these 73 monoamine drugs related to GPCR receptors, and we were interested in discovering unexpected cross-reactivity between completely unrelated protein targets regarding the sequence, functional and structural similarity. Finally, six drugs (Table S4) were selected based on commercial availability and submitted to radio-label competitive binding assay. Among them, one kinase drug, sorafenib (Figure 1), ranks 85 in the original score list, 37 after structural filtering and 9 after activity annotation check.

Sorafenib was purchased from LC Laboratories (Woburn, MA), and the remaining five drug compounds were purchased from Sigma-Aldrich (Table S4). The vendors had verified the compound purity > 95% by liquid chromatography-mass spectrometry (LC-MS) or nuclear magnetic resonance (NMR) experiments. The <sup>1</sup>H-NMR spectrum and LC-MS data for sorafenib are included in Supplementary Materials (Figure S2) to further validate its structure and purity. The primary screening results indicate that two compounds are shown radio-labeled ligand replacement ratio larger than 20% at 10  $\mu$ M concentration and sorafenib exhibits 88% inhibition. Subsequent secondary dose-response experiments indicate that sorafenib binds to 5-HT<sub>2A</sub> with  $K_i$  value of 1959 nM (Figure 7). The cellular functional assay validated sorafenib as a 5-HT<sub>2A</sub> antagonist with 93.3 $\pm$ 1.4% of inhibition activity at 50  $\mu$ M concentration. Remarkably, further 5-HTR profiling results suggest that sorafenib is a promiscuous 5-HTR ligand (Table 2), strongly binds to 5-HT<sub>2B</sub> and 5-HT<sub>2C</sub> with  $K_i$  values of 56 and 417 nM (Figure 7), and weakly binds to other five 5-HTRs including 5-HT<sub>1A</sub>, 5-HT<sub>2A</sub>, 5-HT<sub>5a</sub>, 5-HT<sub>6</sub> and 5-HT<sub>7</sub>, while it doesn't bind to 5-HT<sub>1B</sub>, 5-HT<sub>1E</sub>, 5-HT<sub>1F</sub> and 5-HT<sub>3</sub>. Although at the current stage, it is not clearly whether sorafenib binds to other monoaminergic GPCRs, but it is highly likely to do so considering the ligand promiscuity among the monoaminergic GPCR family.

### 5-HT<sub>2A</sub>-Sorafenib Binding Mode

Here we examine in more depth the docked complex structure of sorafenib focusing on its chemical composition and binding mode (Figure 8A). Compared to the predicted ketanserin and cyproheptadine binding modes, sorafenib has very different binding characteristics regarding its numerous polar interactions with binding-site residues. Its hydrophobic trifluoromethylphenyl unit is buried in the hydrophobic site 1, and might contribute largely to ligand binding. Remarkably, it doesn't contain a positively charged nitrogen atom; instead, it forms strong hydrogen bonds between amide nitrogen atoms of its urea moiety to the carboxylate group of D<sub>3.32</sub>. Other polar interactions include hydrogen bonds between its methyl amide oxygen atom to the hydroxyl group of T<sub>2.64</sub> and amide nitrogen atom of Asn<sub>7.36</sub>, also its methyl amide nitrogen donates a hydrogen bond to the main chain carbonyl of L<sub>7.35</sub>. It is interesting that the amide nitrogen atoms of the urea moiety form exactly the same interaction with the carboxylate group of the residue E500 in sorafenib-kinase crystal complex structures.<sup>72</sup> The binding details of sorafenib with BRAF kinase (PDB code: 1UWH) are illustrated in Figure 8B. It is not likely that the lack of a positively charged group largely reduces the binding affinity between sorafenib and 5-HT<sub>2A</sub>, as its binding to 5-HT<sub>2B</sub> is at low nanomolar range, where this selectivity may be caused by the other



variable binding-site residues like the 5.46 position residue (a serine in 5-HT<sub>2A</sub>, while an alanine in 5-HT<sub>2B</sub> and 5-HT<sub>2C</sub>) just as the ergoline compounds<sup>70</sup>. This is consistent with a recent report where Ladduwahetty and coworkers discovered novel 5-HT<sub>2A</sub> receptor antagonists without containing any positively charged groups<sup>73</sup>. Nevertheless, it is likely that sorafenib can be used as a novel 5-HT<sub>2A</sub> lead compound for further structural optimization with maintaining the bi-aryl urea structural moiety. As the ligand similarity-based SEA method has been successfully applied in identifying GPCR related off-targets, the receptor structure-based docking method may become a complementary approach for GPCR drug off-target discovery when the receptor structure is available or can be reliably modeled. Nevertheless, well designed experimental mutagenesis studies and the development of more accurate 5-HT<sub>2A</sub>-sorafenib structure models are desirable for further investigation of the binding details at the atomic level.

As a proof-of-concept study, we designed series of sorafenib analogues to assess the predicted binding mode; two of them (Figure 9A) have been synthesized and evaluated against 5-HT<sub>2B</sub> receptor (Figure 9B). The chemical synthesis route and analysis data are reported in Supplementary Material. The replacement of aromatic nitrogen atom to carbon atom in compound HN01, leads to slight improvement of binding, which indicates that the aromatic nitro atom doesn't form direct polar interaction with receptor. The addition of methyl group on amide nitrogen atom in compound HN02 removes its potential hydrogen bond to the main chain carbonyl of L<sub>7.35</sub>, leads to 8 folds loss of binding. Both modifications strongly support the predicted binding mode of sorafenib. The complete SAR exploration on sorafenib will be pursued and published at somewhere else.

### New Clinical Implication of Sorafenib

Sorafenib is well known to produce anticancer effect through targeting multiple kinases. Sorafenib was originally developed as a RAF-kinase inhibitor (52 nM), but subsequently has been shown to be a multi-kinase inhibitor that also inhibits PDGFR $\beta$  (37 nM), VEGFR2 (59 nM), VEGFR3 (16 nM), c-Kit (31 nM) and FLT1 (31 nM).<sup>74</sup> 5-HT<sub>2B</sub> is highly expressed in the liver, kidneys, stomach and gut.<sup>12</sup> Considering that the 5-HT<sub>2B</sub> binding affinity of sorafenib is in the same therapeutic window as its kinase inhibition activities, one may hypothesize that the 5-HT<sub>2B</sub> inhibition might directly contribute to the anticancer effect of sorafenib; in this regard we have previously suggested that 5-HT<sub>2B</sub> antagonists might be of special benefit for carcinoid tumors and sorafenib might represent a novel treatment for this disorder.<sup>75</sup> Nevertheless, recent studies have suggested that 5-HT receptors may be involved in the cell viability and cell cycle progression in certain cancers, especially for liver cancer and carcinoid-like tumors.<sup>76-78</sup> Sorafenib was approved to treat advanced renal cell carcinoma (RCC) and hepatocellular carcinoma (HCC), and intriguingly, 5-HT was suggested to promote cell survival and growth of HCC cells by activation of the 5-HT<sub>2B</sub> receptor.<sup>78</sup> However, we cannot exclude the possibility that the 5-HTR activities of sorafenib might also cause side effects instead of bringing clinical benefits in certain circumstances. Although, it is well beyond the scope of our current study, it is desirable to dissect the contributions of kinase inhibitions and 5-HTR antagonist activities in sorafenib-produced anticancer effect; as such information may facilitate clinical usage of sorafenib as well as designing new drugs with better anticancer efficacy and fewer side effects.

## 4. CONCLUSION

Drug profiling campaigns have revealed novel polypharmacology of existing drugs. It is critical to fully understand the target binding profile of a drug molecule, as its potential off-target binding properties may lead to better clinical efficacy in certain circumstances, while causing side effects in other cases. GPCRs and kinases are two of the most important drug target families, and many of their ligands have been discovered to have promiscuous binding

propensities within their own protein families. However, as far as we are aware, the ligand cross-reactivity between GPCR orthosteric ligand and kinase inhibitor has not been previously reported.

To predict novel polypharmacology, we computationally screened the FDA approved drug molecules against the induced-fit models of the 5-HT<sub>2A</sub> receptor. We employed a comprehensive “induced-fit” protocol to simulate the receptor conformational changes upon binding with two representative 5-HT<sub>2A</sub> antagonists, where different computational techniques were integrated systematically, including homology modeling, molecular docking, sidechain prediction and molecular dynamics in explicit membrane and solvent conditions. The multiple independent simulations with the presence of different ligand docking poses lead to the best quality structural models which satisfy the available experimental evidences, and achieve the best docking performance by enriching the known ligands from decoy molecules in retrospective virtual screening. Such identified induced-fit models were used in docking screening of FDA drug molecules, with a total of six drug molecules chosen for experimental binding assay. Surprisingly, a well known multi-kinase inhibitor, sorafenib has shown relatively strong binding affinity to 5-HT<sub>2A</sub>, and subsequent 5-HTR profiling results indicate its promiscuous 5-HTRs inhibition activities. Whether or not the off-target inhibition of 5-HTRs by sorafenib has any clinical relevance has yet to be determined. However, it is desirable to dissect the contributions of kinase inhibitions and 5-HTR antagonist activities in sorafenib-produced anticancer effects. Ultimately, we can also envision a strategy to virtual screening GPCR ligands against therapeutically relevant kinases, and ask whether we could discover known GPCR ligands with unexpected kinase activities.

Interestingly, the structural characteristics of sorafenib are distinct to classic 5-HT<sub>2A</sub> antagonists, especially considering the lack of the tertiary amine to form the salt-bridge interaction with the critical binding-site residue D<sub>3.32</sub>. Instead, sorafenib may form strong hydrogen bonds between amide nitrogen atoms of its urea moiety to carboxylate group of D<sub>3.32</sub>, and it may also form additional hydrogen bonds between its methyl amide with binding-site residues. Nevertheless, the biaryl urea moiety may suggest new direction for developing novel 5-HTR ligands.

## Supplementary Material

Refer to Web version on PubMed Central for supplementary material.

## Acknowledgments

We thank the anonymous reviewers for their constructive comments for improving the manuscript. Financial support from the Chinese Ministry of Science and Technology “973” Grant 2011CB812402 (to NH) is gratefully acknowledged. BLR, RW and X-PH were supported by RO1MH82441 and the NIMH Psychoactive Drug Screening Program (PDSP). Computational support was provided by the Supercomputing Center of Chinese Academy of Sciences (SCCAS) and the Beijing Computing Center (BCC). We also thank Dr. Pearl Huang at BeiGene LTD for reading the manuscript and advice, and Dr. Andrew Christofferson for proofreading.

## ABBREVIATIONS

<b>CNS</b>	central nervous system
<b>GPCRs</b>	G protein-coupled receptors
<b>5-HTRs</b>	5-hydroxytryptamine receptors
<b>β2-AR</b>	β2-adrenoceptor

<b>ECL2</b>	extracellular loop 2
<b>TM</b>	transmembrane helix
<b>PLOP</b>	Protein Local Optimization Program
<b>MD</b>	molecular dynamics
<b>PME</b>	Particle Mesh Ewald
<b>RMSDs</b>	root-mean-square differences
<b>SEA</b>	Similarity Ensemble Approach
<b>PDSP</b>	Psychoactive Drug Screening Program
<b>SAR</b>	structure-activity relationship
<b>EF</b>	enrichment factor
<b>LC-MS</b>	liquid chromatography-mass spectrometry
<b>NMR</b>	nuclear magnetic resonance
<b>RCC</b>	advanced renal cell carcinoma
<b>HCC</b>	hepatocellular carcinoma

## References

1. Roth BL, Sheffler DJ, Kroeze WK. Magic shotguns versus magic bullets: selectively non-selective drugs for mood disorders and schizophrenia. *Nat Rev Drug Discov.* 2004; 3:353–359. [PubMed: 15060530]
2. Sams-Dodd F. Target-based drug discovery: is something wrong? *Drug Discovery Today.* 2005; 10:139–147. [PubMed: 15718163]
3. Weber A, Casini A, Heine A, Kuhn D, Supuran CT, Scozzafava A, Klebe G. Unexpected nanomolar inhibition of carbonic anhydrase by COX-2-selective celecoxib: new pharmacological opportunities due to related binding site recognition. *J Med Chem.* 2004; 47:550–557. [PubMed: 14736236]
4. Capdeville R, Buchdunger E, Zimmermann J, Matter A. Glivec (STI571, imatinib), a rationally developed, targeted anticancer drug. *Nat Rev Drug Discov.* 2002; 1:493–502. [PubMed: 12120256]
5. Fabian MA, Biggs WH 3rd, Treiber DK, Atteridge CE, Azimioara MD, Benedetti MG, Carter TA, Ciceri P, Edeen PT, Floyd M, Ford JM, Galvin M, Gerlach JL, Grotzfeld RM, Herrgard S, Insko DE, Insko MA, Lai AG, Lelias JM, Mehta SA, Milanov ZV, Velasco AM, Wodicka LM, Patel HK, Zarrinkar PP, Lockhart DJ. A small molecule-kinase interaction map for clinical kinase inhibitors. *Nat Biotechnol.* 2005; 23:329–336. [PubMed: 15711537]
6. Xie L, Wang J, Bourne PE. In silico elucidation of the molecular mechanism defining the adverse effect of selective estrogen receptor modulators. *PLoS Comput Biol.* 2007; 3:e217. [PubMed: 18052534]
7. Keiser MJ, Roth BL, Armbruster BN, Ernsberger P, Irwin JJ, Shoichet BK. Relating protein pharmacology by ligand chemistry. *Nat Biotechnol.* 2007; 25:197–206. [PubMed: 17287757]
8. Liu X, Ouyang S, Yu B, Liu Y, Huang K, Gong J, Zheng S, Li Z, Li H, Jiang H. PharmMapper server: a web server for potential drug target identification using pharmacophore mapping approach. *Nucleic Acids Res.* 2009; 38(Suppl):W609–614. [PubMed: 20430828]
9. Yang L, Chen J, Shi L, Hudock MP, Wang K, He L. Identifying unexpected therapeutic targets via chemical-protein interactome. *PLoS One.* 2010; 5:e9568. [PubMed: 20221449]
10. Yadav PN, Kroeze WK, Farrell MS, Roth BL. Antagonist functional selectivity: 5-HT<sub>2A</sub> serotonin receptor antagonists differentially regulate 5-HT<sub>2A</sub> receptor protein level *in vivo*. *J Pharmacol Exp Ther.* 2011; 339:99–105. [PubMed: 21737536]

11. Lowrie JF, Delisle RK, Hobbs DW, Diller DJ. The different strategies for designing GPCR and kinase targeted libraries. *Comb Chem High Throughput Screen*. 2004; 7:495–510. [PubMed: 15320714]
12. Nichols DE, Nichols CD. Serotonin receptors. *Chem Rev*. 2008; 108:1614–1641. [PubMed: 18476671]
13. Sharpley AL, Elliott JM, Attenburrow MJ, Cowen PJ. Slow wave sleep in humans: role of 5-HT<sub>2A</sub> and 5-HT<sub>2C</sub> receptors. *Neuropharmacology*. 1994; 33:467–471. [PubMed: 7984285]
14. Salmi P, Ahlenius S. Evidence for functional interactions between 5-HT<sub>1A</sub> and 5-HT<sub>2A</sub> receptors in rat thermoregulatory mechanisms. *Pharmacol Toxicol*. 1998; 82:122–127. [PubMed: 9553989]
15. Nacmias B, Ricca V, Tedde A, Mezzani B, Rotella CM, Sorbi S. 5-HT<sub>2A</sub> receptor gene polymorphisms in anorexia nervosa and bulimia nervosa. *Neurosci Lett*. 1999; 277:134–136. [PubMed: 10624828]
16. Nagatomo T, Rashid M, Abul Muntasir H, Komiyama T. Functions of 5-HT<sub>2A</sub> receptor and its antagonists in the cardiovascular system. *Pharmacol Ther*. 2004; 104:59–81. [PubMed: 15500909]
17. Roth BL, Willins DL, Kristiansen K, Kroeze WK. 5-Hydroxytryptamine<sub>2</sub>-family receptors (5-hydroxytryptamine<sub>2A</sub>, 5-hydroxytryptamine<sub>2B</sub>, 5-hydroxytryptamine<sub>2C</sub>): where structure meets function. *Pharmacol Ther*. 1998; 79:231–257. [PubMed: 9776378]
18. Rowley M, Bristow LJ, Hutson PH. Current and novel approaches to the drug treatment of schizophrenia. *J Med Chem*. 2001; 44:477–501. [PubMed: 11170639]
19. Congreve M, Langmead CJ, Mason JS, Marshall FH. Progress in structure based drug design for G protein-coupled receptors. *J Med Chem*. 2011; 54:4283–4311. [PubMed: 21615150]
20. Palczewski K, Kumasaka T, Hori T, Behnke CA, Motoshima H, Fox BA, Le Trong I, Teller DC, Okada T, Stenkamp RE, Yamamoto M, Miyano M. Crystal structure of rhodopsin: A G protein-coupled receptor. *Science*. 2000; 289:739–745. [PubMed: 10926528]
21. Congreve M, Marshall F. The impact of GPCR structures on pharmacology and structure-based drug design. *Br J Pharmacol*. 2009; 159:986–996. [PubMed: 19912230]
22. Li YY, Hou TJ, Goddard WA 3rd. Computational modeling of structure-function of g protein-coupled receptors with applications for drug design. *Curr Med Chem*. 2010; 17:1167–1180. [PubMed: 20158474]
23. Costanzi S. On the applicability of GPCR homology models to computer-aided drug discovery: a comparison between in silico and crystal structures of the beta<sub>2</sub>-adrenergic receptor. *J Med Chem*. 2008; 51:2907–2914. [PubMed: 18442228]
24. Senderowitz H, Marantz Y. G Protein-Coupled Receptors: target-based in silico screening. *Curr Pharm Des*. 2009; 15:4049–4068. [PubMed: 20028321]
25. Mobarec JC, Sanchez R, Filizola M. Modern homology modeling of G-protein coupled receptors: which structural template to use? *J Med Chem*. 2009; 52:5207–5216. [PubMed: 19627087]
26. Yarnitzky T, Levit A, Niv MY. Homology modeling of G-protein-coupled receptors with X-ray structures on the rise. *Curr Opin Drug Discov Devel*. 2010; 13:317–325.
27. Phatak SS, Gatica EA, Cavasotto CN. Ligand-steered modeling and docking: A benchmarking study in class A G-protein-coupled receptors. *J Chem Inf Model*. 2010; 50:2119–2128. [PubMed: 21080692]
28. McRobb FM, Capuano B, Crosby IT, Chalmers DK, Yuriev E. Homology modeling and docking evaluation of aminergic G protein-coupled receptors. *J Chem Inf Model*. 2010; 50:626–637. [PubMed: 20187660]
29. Carlsson J, Coleman RG, Setola V, Irwin JJ, Fan H, Schlessinger A, Sali A, Roth BL, Shoichet BK. Ligand discovery from a dopamine D<sub>3</sub> receptor homology model and crystal structure. *Nat Chem Biol*. 2011; 7:769–778. [PubMed: 21926995]
30. Hanson MA, Cherezov V, Griffith MT, Roth CB, Jaakola VP, Chien EY, Velasquez J, Kuhn P, Stevens RC. A specific cholesterol binding site is established by the 2.8 Å structure of the human beta<sub>2</sub>-adrenergic receptor. *Structure*. 2008; 16:897–905. [PubMed: 18547522]
31. Sali A, Blundell TL. Comparative protein modelling by satisfaction of spatial restraints. *J Mol Biol*. 1993; 234:779–815. [PubMed: 8254673]

32. Horn F, Weare J, Beukers MW, Horsch S, Bairoch A, Chen W, Edvardsen O, Campagne F, Vriend G. GPCRDB: an information system for G protein-coupled receptors. *Nucleic Acids Res.* 1998; 26:275–279. [PubMed: 9399852]
33. Marchler-Bauer A, Lu S, Anderson JB, Chitsaz F, Derbyshire MK, DeWeese-Scott C, Fong JH, Geer LY, Geer RC, Gonzales NR, Gwadz M, Hurwitz DI, Jackson JD, Ke Z, Lanczycki CJ, Lu F, Marchler GH, Mullokandov M, Omelchenko MV, Robertson CL, Song JS, Thanki N, Yamashita RA, Zhang D, Zhang N, Zheng C, Bryant SH. CDD: a Conserved Domain Database for the functional annotation of proteins. *Nucleic Acids Res.* 2010; 39:D225–229. [PubMed: 21109532]
34. Varady J, Wu X, Fang X, Min J, Hu Z, Levant B, Wang S. Molecular modeling of the three-dimensional structure of dopamine 3 (D3) subtype receptor: discovery of novel and potent D3 ligands through a hybrid pharmacophore- and structure-based database searching approach. *J Med Chem.* 2003; 46:4377–4392. [PubMed: 14521403]
35. Evers A, Klabunde T. Structure-based drug discovery using GPCR homology modeling: successful virtual screening for antagonists of the alpha1A adrenergic receptor. *J Med Chem.* 2005; 48:1088–1097. [PubMed: 15715476]
36. Sherman W, Day T, Jacobson MP, Friesner RA, Farid R. Novel procedure for modeling ligand/receptor induced fit effects. *J Med Chem.* 2006; 49:534–553. [PubMed: 16420040]
37. Evers A, Klebe G. Ligand-supported homology modeling of g-protein-coupled receptor sites: models sufficient for successful virtual screening. *Angew Chem Int Ed Engl.* 2004; 43:248–251. [PubMed: 14695622]
38. Lorber DM, Shoichet BK. Flexible ligand docking using conformational ensembles. *Protein Sci.* 1998; 7:938–950. [PubMed: 9568900]
39. Wei BQ, Baase WA, Weaver LH, Matthews BW, Shoichet BK. A model binding site for testing scoring functions in molecular docking. *J Mol Biol.* 2002; 322:339–355. [PubMed: 12217695]
40. Gloriam DE, Foord SM, Blaney FE, Garland SL. Definition of the G protein-coupled receptor transmembrane bundle binding pocket and calculation of receptor similarities for drug design. *J Med Chem.* 2009; 52:4429–4442. [PubMed: 19537715]
41. Huang N, Shoichet BK, Irwin JJ. Benchmarking Sets for Molecular Docking. *J Med Chem.* 2006; 49:6789–6801. [PubMed: 17154509]
42. Irwin JJ, Shoichet BK, Mysinger MM, Huang N, Colizzi F, Wassam P, Cao Y. Automated docking screens: a feasibility study. *J Med Chem.* 2009; 52:5712–5720. [PubMed: 19719084]
43. Lorber DM, Shoichet BK. Hierarchical docking of databases of multiple ligand conformations. *Curr Top Med Chem.* 2005; 5:739–749. [PubMed: 16101414]
44. Ester, M.; Kriegel, HP.; Sander, J.; Xu, XW. A density-based algorithm for discovering clusters in large spatial databases with noise. In: Simoudis, Evangelos; Han, Jiawei; Fayyad, Usama M., editors. *Proceedings of the Second International Conference on Knowledge Discovery and Data Mining.* AAAI Press; 1995. p. 226-231.
45. Bernacki K, Kalyanaraman C, Jacobson MP. Virtual ligand screening against Escherichia coli dihydrofolate reductase: improving docking enrichment using physics-based methods. *J Biomol Screen.* 2005; 10:675–681. [PubMed: 16170049]
46. Kalyanaraman C, Bernacki K, Jacobson MP. Virtual screening against highly charged active sites: Identifying substrates of alpha-beta barrel enzymes. *Biochemistry.* 2005; 44:2059–2071. [PubMed: 15697231]
47. Huang N, Kalyanaraman C, Bernacki K, Jacobson MP. Molecular mechanics methods for predicting protein-ligand binding. *Phys Chem Chem Phys.* 2006; 8:5166–5177. [PubMed: 17203140]
48. Huang N, Kalyanaraman C, Irwin JJ, Jacobson MP. Physics-based scoring of protein-ligand complexes: enrichment of known inhibitors in large-scale virtual screening. *J Chem Inf Model.* 2006; 46:243–253. [PubMed: 16426060]
49. Huang N, Jacobson MP. Binding-site assessment by virtual fragment screening. *PLoS One.* 2010; 5:e10109. [PubMed: 20404926]
50. Rapp CS, Schonbrun C, Jacobson MP, Kalyanaraman C, Huang N. Automated site preparation in physics-based rescoring of receptor ligand complexes. *Proteins.* 2009; 77:52–61. [PubMed: 19382204]



51. Jacobson MP, Kaminski GA, Friesner RA, Rapp CA. Force field validation using protein side chain prediction. *J Phys Chem B*. 2002; 106:11673–11680.
52. Jacobson MP, Pincus DL, Rapp CS, Day TJ, Honig B, Shaw DE, Friesner RA. A hierarchical approach to all-atom protein loop prediction. *Proteins*. 2004; 55:351–367. [PubMed: 15048827]
53. Li X, Jacobson MP, Friesner RA. High-resolution prediction of protein helix positions and orientations. *Proteins*. 2004; 55:368–382. [PubMed: 15048828]
54. Kevin, JB.; Edmond, C.; Huafeng, X.; Ron, OD.; Michael, PE.; Brent, AG.; John, LK.; István, K.; Mark, AM.; Federico, DS.; John, KS.; Yibing, S.; David, ES. Scalable algorithms for molecular dynamics simulations on commodity clusters. *Proceedings of the ACM/IEEE Conference on Supercomputing (SC06)*; Tampa, Florida. November 11–17, 2006;
55. Banks JL, Beard HS, Cao Y, Cho AE, Damm W, Farid R, Felts AK, Halgren TA, Mainz DT, Maple JR, Murphy R, Philipp DM, Repasky MP, Zhang LY, Berne BJ, Friesner RA, Gallicchio E, Levy RM. Integrated Modeling Program, Applied Chemical Theory (IMPACT). *J Comput Chem*. 2005; 26:1752–1780. [PubMed: 16211539]
56. Kräutler V, van Gunsteren WF, Hünenberger PH. A fast SHAKE algorithm to solve distance constraint equations for small molecules in molecular dynamics simulations. *J Comput Chem*. 2001; 22:501–508.
57. Darden T, York D, Pedersen L. Particle mesh Ewald: An  $N \log(N)$  method for Ewald sums in large systems. *J Chem Phys*. 1993; 98:10089–10092.
58. Pettersen EF, Goddard TD, Huang CC, Couch GS, Greenblatt DM, Meng EC, Ferrin TE. UCSF Chimera--a visualization system for exploratory research and analysis. *J Comput Chem*. 2004; 25:1605–1612. [PubMed: 15264254]
59. Humphrey W, Dalke A, Schulten K. VMD: visual molecular dynamics. *J Mol Graph*. 1996; 14:33–38. [PubMed: 8744570]
60. Irwin JJ, Shoichet BK. ZINC--a free database of commercially available compounds for virtual screening. *J Chem Inf Model*. 2005; 45:177–182. [PubMed: 15667143]
61. Wishart DS, Knox C, Guo AC, Shrivastava S, Hassanali M, Stothard P, Chang Z, Woolsey J. DrugBank: a comprehensive resource for in silico drug discovery and exploration. *Nucleic Acids Res*. 2006; 34:D668–672. [PubMed: 16381955]
62. Overington J. ChEMBL. An interview with John Overington, team leader, chemogenomics at the European Bioinformatics Institute Outstation of the European Molecular Biology Laboratory (EMBL-EBI). Interview by Wendy A. Warr. *J Comput Aided Mol Des*. 2009; 23:195–198. [PubMed: 19194660]
63. Keiser MJ, Setola V, Irwin JJ, Laggner C, Abbas AI, Hufeisen SJ, Jensen NH, Kuijter MB, Matos RC, Tran TB, Whaley R, Glennon RA, Hert J, Thomas KL, Edwards DD, Shoichet BK, Roth BL. Predicting new molecular targets for known drugs. *Nature*. 2009; 462:175–181. [PubMed: 19881490]
64. Surgand JS, Rodrigo J, Kellenberger E, Rognan D. A chemogenomic analysis of the transmembrane binding cavity of human G-protein-coupled receptors. *Proteins*. 2006; 62:509–538. [PubMed: 16294340]
65. Runyon SP, Mosier PD, Roth BL, Glennon RA, Westkaemper RB. Potential modes of interaction of 9-aminomethyl-9,10-dihydroanthracene (AMDA) derivatives with the 5-HT<sub>2A</sub> receptor: a ligand structure-affinity relationship, receptor mutagenesis and receptor modeling investigation. *J Med Chem*. 2008; 51:6808–6828. [PubMed: 18847250]
66. Shi L, Javitch JA. The binding site of aminergic G protein-coupled receptors: the transmembrane segments and second extracellular loop. *Annu Rev Pharmacol Toxicol*. 2002; 42:437–467. [PubMed: 11807179]
67. Roth BL, Shoham M, Choudhary MS, Khan N. Identification of conserved aromatic residues essential for agonist binding and second messenger production at 5-hydroxytryptamine<sub>2A</sub> receptors. *Mol Pharmacol*. 1997; 52:259–266. [PubMed: 9271348]
68. Choudhary MS, Craigo S, Roth BL. A single point mutation (Phe340-->Leu340) of a conserved phenylalanine abolishes 4-[125I]iodo-(2,5-dimethoxy)phenylisopropylamine and [3H]mesulergine but not [3H]ketanserin binding to 5-hydroxytryptamine<sub>2</sub> receptors. *Mol Pharmacol*. 1993; 43:755–761. [PubMed: 8388989]

69. Almaula N, Ebersole BJ, Zhang D, Weinstein H, Sealfon SC. Mapping the binding site pocket of the serotonin 5-Hydroxytryptamine<sub>2A</sub> receptor. Ser3.36(159) provides a second interaction site for the protonated amine of serotonin but not of lysergic acid diethylamide or bufotenin. *J Biol Chem.* 1996; 271:14672–14675. [PubMed: 8663249]
70. Almaula N, Ebersole BJ, Ballesteros JA, Weinstein H, Sealfon SC. Contribution of a helix 5 locus to selectivity of hallucinogenic and nonhallucinogenic ligands for the human 5-hydroxytryptamine<sub>2A</sub> and 5-hydroxytryptamine<sub>2C</sub> receptors: direct and indirect effects on ligand affinity mediated by the same locus. *Mol Pharmacol.* 1996; 50:34–42. [PubMed: 8700116]
71. Westkaemper RB, Glennon RA. Application of ligand SAR, receptor modeling and receptor mutagenesis to the discovery and development of a new class of 5-HT<sub>2A</sub> ligands. *Curr Top Med Chem.* 2002; 2:575–598. [PubMed: 12052195]
72. Wan PT, Garnett MJ, Roe SM, Lee S, Niculescu-Duvaz D, Good VM, Jones CM, Marshall CJ, Springer CJ, Barford D, Marais R. Mechanism of activation of the RAF-ERK signaling pathway by oncogenic mutations of B-RAF. *Cell.* 2004; 116:855–867. [PubMed: 15035987]
73. Ladduwahetty T, Gilligan M, Humphries A, Merchant KJ, Fish R, McAlister G, Ivarsson M, Dominguez M, O'Connor D, MacLeod AM. Non-basic ligands for aminergic GPCRs: the discovery and development diaryl sulfones as selective, orally bioavailable 5-HT<sub>2A</sub> receptor antagonists for the treatment of sleep disorders. *Bioorg Med Chem Lett.* 2010; 20:3708–3712. [PubMed: 20493697]
74. Karaman MW, Herrgard S, Treiber DK, Gallant P, Atteridge CE, Campbell BT, Chan KW, Ciceri P, Davis MI, Edeen PT, Faraoni R, Floyd M, Hunt JP, Lockhart DJ, Milanov ZV, Morrison MJ, Pallares G, Patel HK, Pritchard S, Wodicka LM, Zarrinkar PP. A quantitative analysis of kinase inhibitor selectivity. *Nat Biotechnol.* 2008; 26:127–132. [PubMed: 18183025]
75. Roth BL. Drugs and valvular heart disease. *N Engl J Med.* 2007; 356:6–9. [PubMed: 17202450]
76. Oufkir T, Arseneault M, Sanderson JT, Vaillancourt C. The 5-HT<sub>2A</sub> serotonin receptor enhances cell viability, affects cell cycle progression and activates MEK-ERK1/2 and JAK2-STAT3 signalling pathways in human choriocarcinoma cell lines. *Placenta.* 2010; 31:439–447. [PubMed: 20338635]
77. Asada M, Ebihara S, Yamanda S, Niu K, Okazaki T, Sora I, Arai H. Depletion of serotonin and selective inhibition of 2B receptor suppressed tumor angiogenesis by inhibiting endothelial nitric oxide synthase and extracellular signal-regulated kinase 1/2 phosphorylation. *Neoplasia.* 2009; 11:408–417. [PubMed: 19308295]
78. Soll C, Jang JH, Riener MO, Moritz W, Wild PJ, Graf R, Clavien PA. Serotonin promotes tumor growth in human hepatocellular cancer. *Hepatology.* 2010; 51:1244–1254. [PubMed: 20099302]

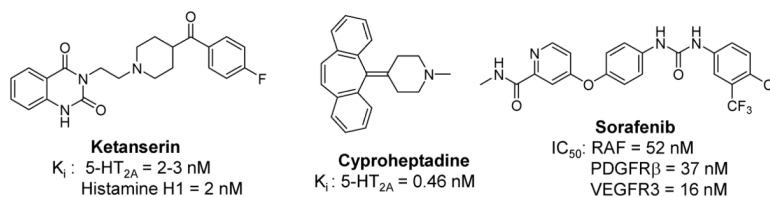


**Figure 1.**  
Chemical structures of ketanserin, cyproheptadine and sorafenib with activity data of their known primary targets.

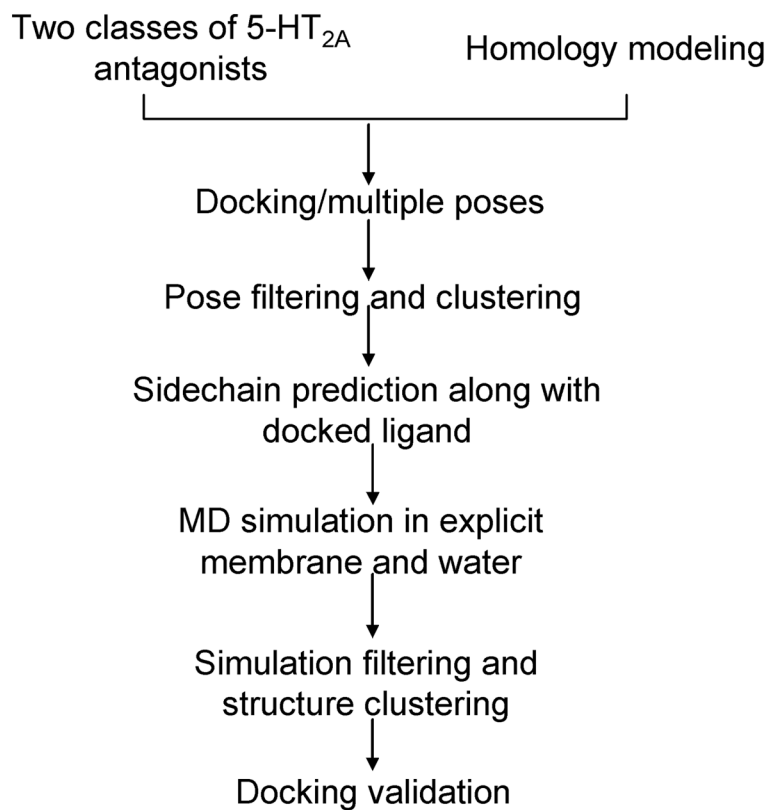


**Figure 2.** Our step-by-step induced-fit protocol to improve the 5-HT<sub>2A</sub> homology model for bound ligands.

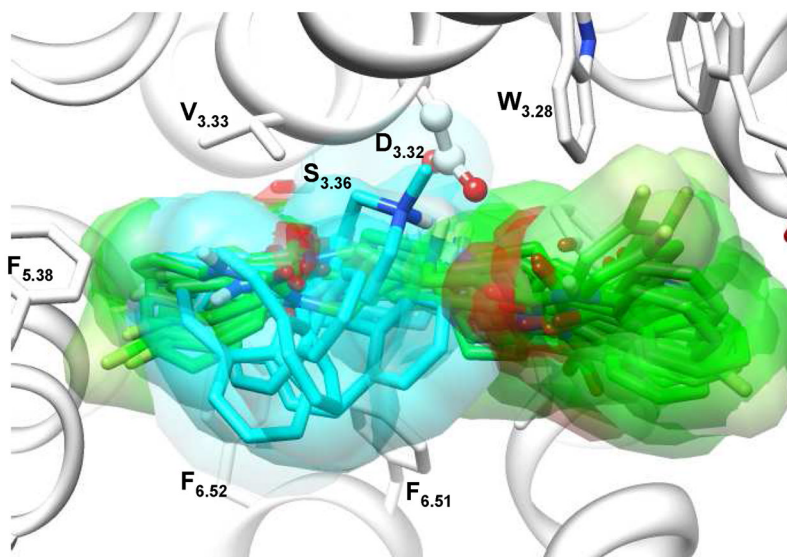


**Figure 3.** Overlapped diverse representative docking poses of ketanserin and cyproheptadine in the binding-site of the initial homology model of 5-HT<sub>2A</sub>. Cyproheptadine (carbon atoms colored cyan) mainly binds in site 1, mainly bordered by TM3, 5 and 6, while ketanserin (colored green) adopts extended conformations that allow binding both sites.



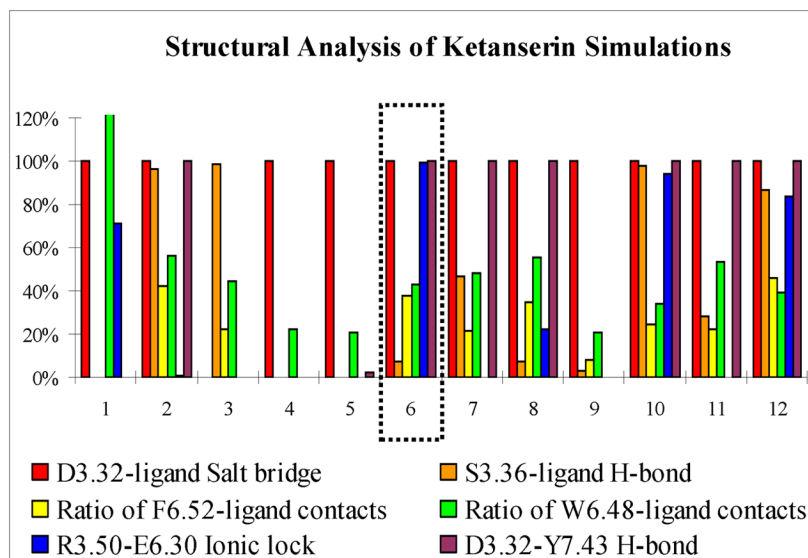


**Figure 4.**

The structural descriptors used to assess the simulation quality of ketanserin complex systems. Y axis is the measured probability of forming a specific interaction during 10 ns production simulation. The formation of D3.32-ligand salt bridge interaction is defined as the distance between carboxylate oxygen atom of D3.32 and the piperidine nitrogen atom of ligand less than 3.5 Å, the hydrogen bond between ligand and hydroxyl of residue S<sub>3,36</sub> is defined by the distance of donor and acceptor less than 3.5 Å and angle greater than 120° (same for D3.32-Y7.43 hydrogen bond), the ratio of F6.52-ligand contacts is defined by the number of atom pairs within vdW contact distance between ligand and F6.52 divided by the number of atom pairs between ligand and F6.51 (same for W6.48-ligand contacts), and the R3.50-E6.30 ionic lock is defined by distance less than 4 Å between CZ atom of R3.50 and CD atom of E6.30.

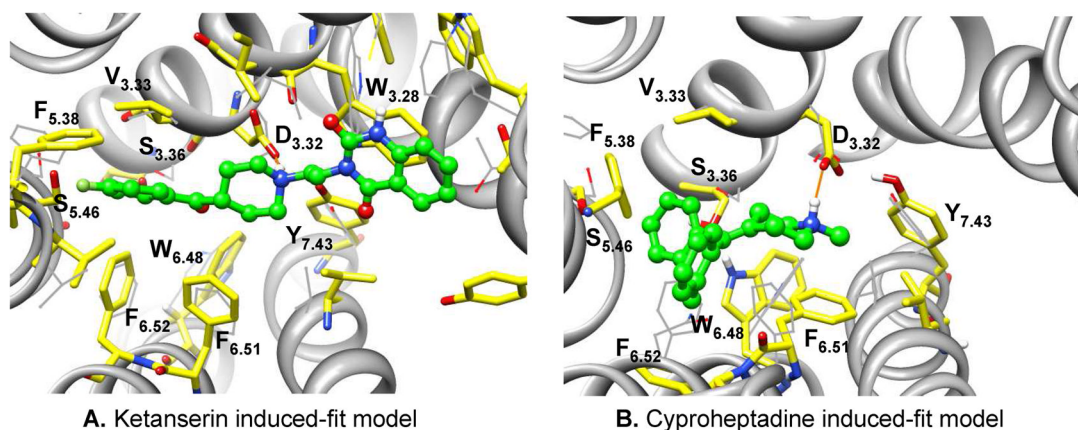


**Figure 5.** Conformational changes upon binding ligands ketanserin (A) and cyproheptadine (B). Induced-fit model (stick, carbon atoms colored yellow) is superimposed on the initial homology model (thin line, carbon atoms colored grey), highlighting the binding-site conformational changes in molecular dynamics simulation. The transmembrane helices in the initial homology model are shown in ribbon representation and are omitted in the induced-fit models for clarity purpose. Carbon atoms of ligands are colored in green. The salt-bridge interaction between the tertiary amine of the ligand and the conserved D3.32 is illustrated with orange line. Molecular images were generated with UCSF Chimera.

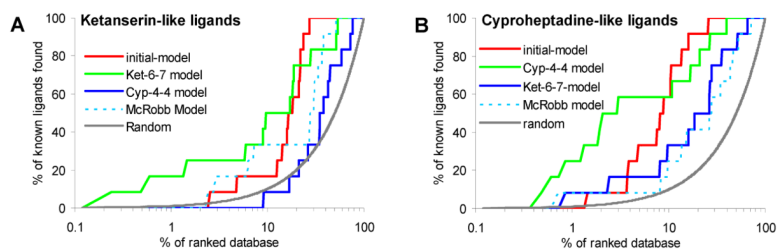


**Figure 6.** The enrichment profile of percentage of ligands found (y-axis) plotted as a function of the percentage of the ranked docked database (x-axis in logarithmic scale).

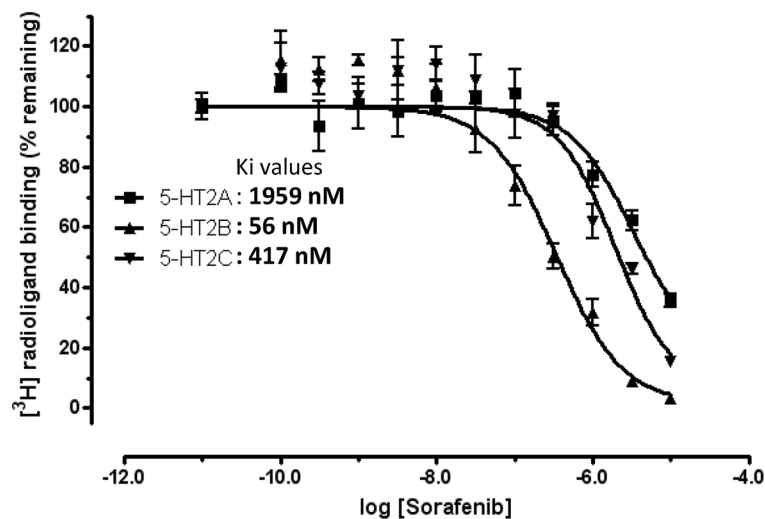


**Figure 7.** Radioligand competition binding assays of sorafenib.  $K_i$  value is calculated as:  $K_i = IC_{50}/(1+L/K_d)$  (Cheng-Prusoff equation), in which [L] = the radioligand concentration used in the binding assay and  $K_d$  is the affinity of radioligand at corresponding receptor. [<sup>3</sup>H]-Ketanserin was used for 5-HT<sub>2A</sub> binding; [<sup>3</sup>H]-LSD for 5-HT<sub>2B</sub> and 5-HT<sub>2C</sub> binding. For 5-HT<sub>2A</sub>, [L] = 3.54 nM and  $K_d$  = 2.2 nM; for 5-HT<sub>2B</sub>, [L] = 2 nM and  $K_d$  = 0.5 nM; for 5-HT<sub>2C</sub>, [L] = 2 nM and  $K_d$  = 0.6 nM.

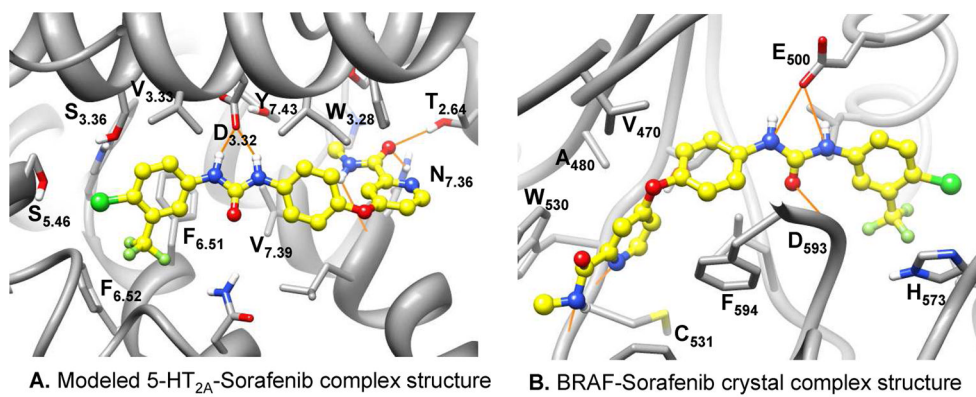


**Figure 8.** The binding mode of sorafenib in the modeled 5-HT<sub>2A</sub>-sorafenib complex structure and the BRAF-sorafenib crystal complex structure. Carbon atoms of sorafenib are colored in yellow. The hydrogen bond interactions between the urea group of the sorafenib and the conserved D3.32 in 5-HT<sub>2A</sub> (A) or the catalytic residue E500 in BRAF (B) are illustrated with orange line. Molecular images were generated with UCSF Chimera.



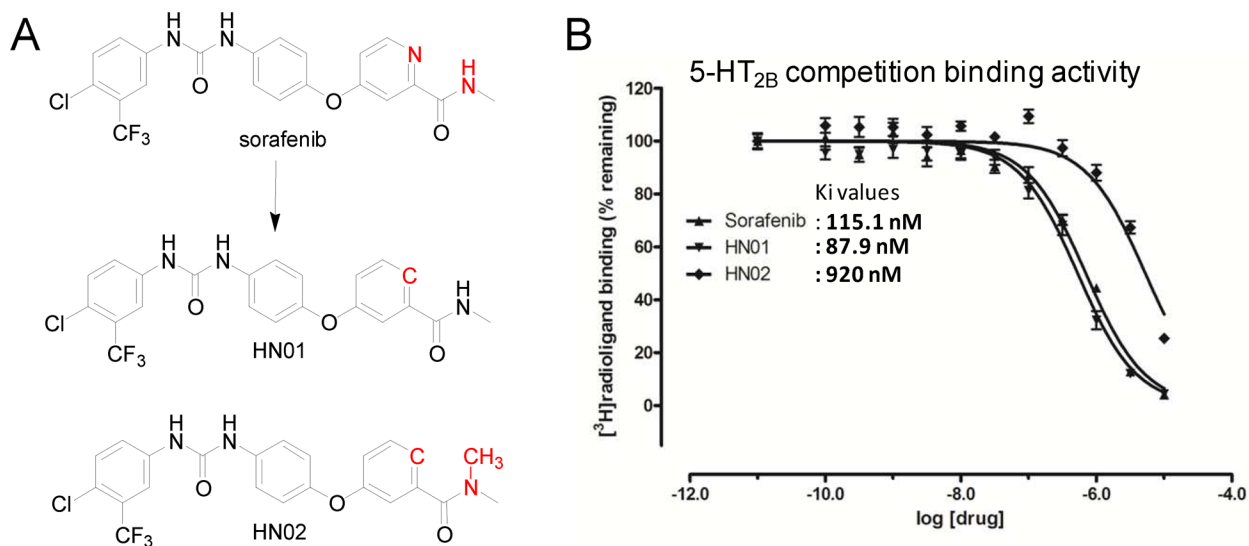


**Figure 9.**

Chemical structures of designed sorafenib analogues (A), and their corresponding radioligand competition binding assay results (B). Note that the measured K<sub>i</sub> value of sorafenib in this binding assay is 115.1 nM, different to our reported value of 56 nM. It is due to a new batch of 5-HT<sub>2B</sub> pellets used in this new assay, where the K<sub>d</sub> value of radioligand [<sup>3</sup>H]-LSD is 0.97 nM, and 0.5 nM for the previously used batch. Thus, the measured sorafenib binding affinity values are consistent in both experiments.

**Table 1**

Enrichments of the 43 5-HT<sub>2A</sub> ligands among a background of 774 “DUD” style decoy molecules by docking against ketanserin and cyproheptadine induced-fit models. EF<sub>1</sub> (enrichment factor at 1% of the ranked database), and EF<sub>5</sub> (enrichment factor at 5% of the database) present the early enrichment performance.

Ket-models	1	2	3	4	5	6	7	8	9	10
EF <sub>1</sub>	2.3	0.0	0.0	0.0	0.0	4.6	4.6	0.0	2.3	0.0
EF <sub>5</sub>	0.5	0.5	0.5	0.0	0.0	1.4	2.3	0.9	0.9	0.9

Cyp-models	1	2	3	4	5	6	7	8	9	10
EF <sub>1</sub>	2.3	0.0	4.6	4.6	1.0	2.3	0.0	2.3	4.6	2.3
EF <sub>5</sub>	1.4	0.9	1.9	3.3	1.0	2.3	2.3	3.3	2.3	1.9

**Table 2**

The 5-HT<sub>1A</sub> binding profile of sorafenib.

Receptor	5-HT <sub>1A</sub>	5-HT <sub>2A</sub>	5-HT <sub>2B</sub>	5-HT <sub>2C</sub>	5-HT <sub>3a</sub>	5-HT <sub>6</sub>	5-HT <sub>7</sub>
Ki (nM)	1,181	1,959	56.0	417.0	3,296	6,213	7,071

Note that data represent Ki (nM) values obtained from non-linear regression of radioligand competition binding isotherms. Ki values are calculated from best fit IC<sub>50</sub> values using the Cheng-Prusoff equation.